Microglial activation precedes acute neurodegeneration in Sandhoff disease and is suppressed by bone marrow transplantation

Ryuichi Wada*, Cynthia J. Tifft*†, and Richard L. Proia*‡

*Genetics of Development and Disease Branch, National Institute of Diabetes and Digestive and Kidney Diseases, National Institutes of Health, Bethesda, MD 20892; and †Department of Medical Genetics, Children's National Medical Center, Washington, DC 20010

Edited by Elizabeth F. Neufeld, University of California, Los Angeles, CA, and approved July 10, 2000 (received for review March 13, 2000)

Sandhoff disease is a lysosomal storage disorder characterized by the absence of β-hexosaminidase and storage of G_{M2} ganglioside and related glycolipids in the central nervous system. The glycolipid storage causes severe neurodegeneration through a poorly understood pathogenic mechanism. In symptomatic Sandhoff disease mice, apoptotic neuronal cell death was prominent in the caudal regions of the brain. cDNA microarray analysis to monitor gene expression during neuronal cell death revealed an upregulation of genes related to an inflammatory process dominated by activated microglia. Activated microglial expansion, based on gene expression and histologic analysis, was found to precede massive neuronal death. Extensive microglia activation also was detected in a human case of Sandhoff disease. Bone marrow transplantation of Sandhoff disease mice suppressed both the explosive expansion of activated microglia and the neuronal cell death without detectable decreases in neuronal G_{M2} ganglioside storage. These results suggest a mechanism of neurodegeneration that includes a vigorous inflammatory response as an important component. Thus, this lysosomal storage disease has parallels to other neurodegenerative disorders, such as Alzheimer's and prion diseases, where inflammatory processes are believed to participate directly in neuronal cell death.

microglia | macrophage | apoptosis | cDNA microarray | tumor necrosis factor-α

Glycolipid storage diseases are caused by inherited defects in enzyme systems necessary for the lysosomal degradation of glycosphingolipids (1). In these disorders, undegraded glycolipids accumulate progressively in lysosomes, eventually triggering pathways leading to cellular dysfunction. In many of the disorders, central nervous system (CNS) dysfunction and degeneration are principal manifestations and the cause of mortality.

Tay-Sachs disease and Sandhoff disease are glycolipid storage diseases caused by the lack of lysosomal β-hexosaminidase (2). In both disorders, G_{M2} ganglioside and related glycolipids—substrates for β-hexosaminidase—accumulate in the nervous system and trigger acute neurodegeneration. In the most severe forms, the onset of symptoms begins in early infancy. A precipitous neurodegenerative course then ensues, with affected infants exhibiting motor dysfunction, seizure, visual loss, and deafness. Death usually occurs by 2–5 years of age. Neuronal loss through an apoptotic mechanism has been demonstrated (3). However, it is not known how excess accumulation of glycolipids ultimately leads to cell death.

Neuronal apoptosis occurs in a number of neurodegenerative diseases, including Alzheimer's disease (4, 5), prion diseases (6, 7), and HIV-dementia (8). In each, an inflammatory process in the CNS is believed to play an important role in the pathway leading to neuronal cell death. The inflammatory response is mediated by microglia—bone marrow-derived cells that normally sense and respond to neuronal damage and remove the damaged cells by phagocytosis (9). However, in pathologic circumstances activated microglia can cause neuronal damage through the expression of inflammatory mediators (6, 10–13).

In this study, we demonstrate an intense CNS inflammatory reaction in both human and murine Sandhoff disease. In mice, activated microglia are present before the acute phase of disease in regions that eventually show a high degree of apoptosis. Bone marrow transplantation (BMT) to introduce normal microglia into the CNS suppressed the expansion of activated microglia and neuronal apoptosis without demonstrable changes in G_{M2} ganglioside storage in neurons. The results are consistent with a model of pathogenesis in which a severe inflammatory response compounds the primary neuronal insult of glycolipid storage and triggers acute neurodegeneration.

Methods

Animals. Sandhoff disease model mice were developed by disruption of the *Hexb* gene as described (14). The *Hexb* genotype was determined by PCR by using mouse-tail DNA and by determination of β-hexosaminidase levels in mouse-tail extracts (14, 15). Bone marrow transplantation was done between 10 and 16 days as described previously (15).

cDNA Microarray Analysis. Pooled spinal cord mRNA samples were obtained from three Sandhoff disease mice and from three strain-matched, wild-type mice. All mice were 4 months old at the time of sacrifice. Total RNA was purified with Trizol solution (GIBCO/BRL). Poly(A) mRNA was purified by using the Qiagen Oligotex mRNA purification kit (Qiagen, Chatsworth, CA). The poly(A) mRNA samples (200 ng) from wild-type and Sandhoff disease mice were labeled with Cy3 and Cy5 fluorescence dyes, respectively, by reverse transcription. Then, the probes were hybridized to the mouse GEM1 microarray (Genome Systems, St. Louis; http://www.genomesystems.com/expression/mousegem1.html). The chip has 8,734 elements representing 7,854 unique mouse genes. Gene expression levels were expressed as a ratio balanced with a coefficient obtained from a control chip.

Quantitative mRNA Analysis by Real-Time PCR. mRNA gene expression levels were determined after reverse transcription by real-time PCR by using an ABI PRISM 7700 Sequence Detection System (Perkin–Elmer). For tumor necrosis factor-α (TNF-α),

This paper was submitted directly (Track II) to the PNAS office.

Abbreviations: BMT, bone marrow transplantation; CNS, central nervous system; TNF-α, tumor necrosis factor-α; TUNEL, terminal deoxynucleotidyltransferase-mediated dUTP nick end labeling; $GSIB_4$, *Griffonia simplicifolia* isolectin B_4.

‡To whom reprint requests should be addressed at: National Institutes of Health, Building 10, Room 9N314, Bethesda, MD 20892. E-mail proia@nih.gov.

The publication costs of this article were defrayed in part by page charge payment. This article must therefore be hereby marked "*advertisement*" in accordance with 18 U.S.C. §1734 solely to indicate this fact.

the TaqMan Pre-Developed Assay Reagent kit for murine TNF-α (Perkin–Elmer) was used. For the genes listed below, the relative expression was determined by using the SYBR Green PCR kit (Perkin–Elmer). The primer sets [Forward (F) and Reverse (R)] used for these assays were: 5′-TTCTGGAAGCCCATTACACAAAC-3′ (B lymphocyte chemoattractant, F), 5′-GCGTAACTTGAATCCGATCTATGAT-3′ (R); 5′-CGACGCCAGCCATTCCT-3′ (Cathepsin S, F), 5′-TCCCATAGCCAACCACAAGAA-3′ (R); 5′-ATGGACAGCTTACCTTTGGATTCA-3′ (CD68, F), 5′-TGCCTGTGGGAAGGACACAT-3′ (R); 5′-AATCGCTGCTGGTTGAATACAG-3′ (F4/80, F), 5′-CCAGGCAAGGAGGACAGAGTT-3′ (R); 5′-AGTATGGTTTCACGTTCATGTGTCA-3′ (Macrophage expressed gene 1, F), 5′-GTGCACCCTCAGCTGTGGTA-3′ (R); 5′-CTCCTGAGTGAGGCTGAAATCA-3′ (Mac-1 alpha subunit, F), 5′-TTATACATCTCCAGCACTGTCTTCGT-3′ (R); 5′-CAGGAAAATGGCAGACAGCTT-3′ [Galectin 3 (Mac-2), F], 5′-CCCATGCACCCGGATATC-3′ (R); 5′-GCTGGTGCCTGACCCATCT-3′ (Secreted phosphoprotein 1, F), 5′-TTCATTGGAATTGCTTGGAAGA-3′ (R); and 5′-AAAACCAGTGTGAGACCAAGATCAT-3′ (Prostaglandin D2 synthetase, F), 5′-CACTGACACGGAGTGGATGCT-3′ (R).

cDNA was synthesized from total RNA by reverse transcriptase reaction by using Superscript II kit (GIBCO/BRL). cDNA synthesized from 1 μg of total RNA for TNF-α and 10 ng of total RNA for other genes was used as template in each reaction. For standardization of quantitation, glyceraldehyde-3-phosphate dehydrogenase was amplified simultaneously. The change of reporter fluorescence from each reaction tube was monitored by ABI PRISM 7700 Sequence Detection System. The threshold cycle of each gene was determined as PCR cycles at which an increase in reporter fluorescence above a baseline signal. The difference in threshold cycles between the target gene and glyceraldehyde-3-phosphate dehydrogenase gives the standardized expression level (dCt). Subtraction of dCt of control mice from dCt of Sandhoff disease mice gives the ddCt value that was used to calculate relative expression levels in Sandhoff disease mice with the formula $2^{-\mathrm{ddCt}}$. The expression levels of each gene were expressed as fold increase in Sandhoff disease mice compared with control mice. Experiments were done in three Sandhoff disease mice and three control mice at 1, 2, 3, and 4 months of age.

Pathology. Three to four Sandhoff disease mice, age-matched control mice at 1, 2, 3, and 4 months of age, and 4-month-old Sandhoff disease mice transplanted with wild-type bone marrow were used for pathologic analysis. The mice were perfused with 10% buffered formalin, and brain and spinal cord were removed. Semisequential coronal sections of the brain (six sections) and spinal cord (eight sections) were made from each mouse and processed for embedding in paraffin. Sections (4 μm thick) were stained with hematoxylin and eosin and used for immunostaining. For frozen sections, brain and spinal cord were obtained from 4-month-old Sandhoff disease mice, control mice, and disease mice transplanted with bone marrow. Tissues were embedded in OCT compound (Sakura Finetek, Torrance, CA) and quickly frozen in liquid nitrogen. Frozen sections (7 μm thick) were prepared with a cryostat. Brain regions were identified based on stereotaxic coordinates.

Apoptosis was detected by *in situ* terminal deoxynucleotidyltransferase-mediated dUTP nick end labeling (TUNEL) method by using an ApopTag kit (Intergen, Purchase, NY).

For immunostaining, paraffinized and rehydrated sections were treated with trypsin and then were incubated with rat anti-F4/80 antibody, rabbit anti-TNF-α antibody (BioSource International, Camarillo, CA), or mouse antiphosphotyrosine antibody (Santa Cruz Biotechnology) overnight at 4°C. The washed sections were incubated with biotinylated anti-rabbit Ig antibody (BioSource International) or anti-rat Ig antibody (Dako) and subsequently incubated with streptavidin–peroxidase complex. Sections for phosphotyrosine detection were incubated with FITC-labeled goat anti-mouse IgG antibody (Sigma). For staining with *Griffonia simplicifolia* isolectin B_4 ($GSIB_4$), deparaffinized sections were incubated with peroxidase-labeled $GSIB_4$ overnight (16). Peroxidase reaction was visualized by diaminobenzidine and hydrogen peroxide. Immunostaining of G_{M2} ganglioside was done on frozen sections of the brain and spinal cord as described (17).

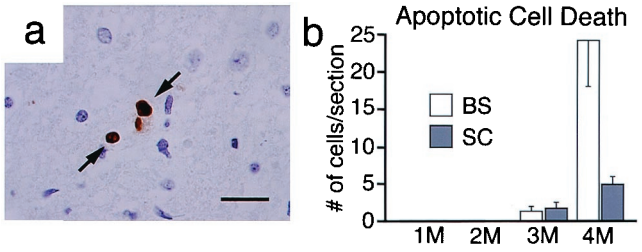

Fig. 1. Apoptosis in Sandhoff disease mice. (*a*) Apoptotic cell death in thalamic nucleus of 4-month-old Sandhoff disease mouse was detected by the *in situ* TUNEL method. (Bar = 20 μm.) (*b*) Incidence of apoptotic cell death in brainstem including thalamic nuclei (BS) and spinal cord (SC) of Sandhoff disease mice. The TUNEL-positive cells were counted in semisequential coronal sections of brain and spinal cord. Data are mean ± SEM (n = 3–4).

Histological and Biochemical Studies on Human Sandhoff Disease. Frozen and paraffin-embedded brain tissues of a 16-month-old Sandhoff disease patient were obtained from The University of Miami, Brain and Tissue Bank for Development Disorders. Specimens from the cerebral cortex, thalamic nucleus, and brainstem of Sandhoff disease patients were used for the study. For control samples, brain specimens from a 9-month-old child who died in an accident were obtained from the Brain and Tissue Bank. Immunostaining of CD68 (Dako) (18) and phosphotyrosine and detection of apoptotic cell death were done described as above. Expression levels of TNF-α mRNA were determined by real-time reverse transcription–PCR, using Pre-Developed TaqMan Assay Reagent kits for human TNF-α and human glyceraldehyde-3-phosphate dehydrogenase (Perkin–Elmer) as described above.

To determine chitotriosidase activity, frozen brain tissues were homogenized in PBS containing 0.5% Triton X-100. Twenty-five microliters of homogenate supernatant was incubated with 100 μl of 0.1 M citric acid/0.2 M sodium phosphate buffer (pH 5.2) containing 22 μM 4-methylumbelliferyl (4-MU)-β-D-*N*,*N*′,*N*″-triacetylchitotrioside (Sigma) at 37°C for an hour (19). Reaction was stopped with 1 ml of 0.2 M glycine/NaOH (pH 10.6). Fluorescent 4-MU was measured with a fluorometer. Protein concentration was determined by the Protein Assay Kit (Bio-Rad). Enzymatic activity was expressed as nanomoles of converted 4-MU per hour per mg protein.

Results

Neuronal Apoptosis. Symptomatic Sandhoff disease mice have been reported to exhibit neuronal apoptosis (3). We surveyed brain regions for apoptotic cells in presymptomatic mice (1 and 2 months of age), in mice at the beginning of an acute decline in motor function (3 months of age), and in severely symptomatic mice (4 months of age) (Fig. 1). During the peak of the disease at 4–4.5 months of age, the mice exhibit tremor, severe ataxia, and muscle weakness. At 1 and 2 months of age, no apoptotic neurons were detected. At 3 months of age, rare apoptotic neurons were detected in the spinal cord, brainstem, and the thalamus. At 4 months of age, the number of apoptotic neurons had increased dramatically in these regions. Apoptotic neurons

Table 1. Genes up-regulated in the spinal cord of Sandhoff disease mice

GenBank accession no.	Expression ratio	Genes
AA152885	**8.0**	**B lymphocyte chemoattractant (BLC)**
AA178121	**5.5**	**Cathepsin S**
AA210495	**5.0**	**Serine protease inhibitor 2-1**
AA051654	4.9	Metallothionein 1
AA2432315	4.7	TYRO protein tyrosine kinase-binding protein
AA423373	4.5	Glycoprotein 49 A
AA220007	**4.5**	**CD68**
AA241784	4.0	Insulin-like growth factor-binding protein 5
AA000461	**4.0**	**Complement component 1, q subcomponent, c polypeptide**
AA259340	3.9	ESTs, weakly similar to retinal short-chain dehydrogenase/reductase
W83447	**3.9**	**Serine protease inhibitor 2-1**
AA277451	3.8	IIGP protein
AA064247	3.7	Metallothionein 1
W89253	3.6	Insulin-like growth factor-binding protein 5
AA267952	3.6	Calcyclin
AA269575	3.5	Nuclear receptor-binding SET-domain protein 1
AA268219	**3.3**	**Macrophage expressed gene 1**
AA178276	**3.2**	**ESTs, moderately similar to Mac-1 α subunit**
AA462611	3.1	ESTs, weakly similar to dual-specificity protein phosphatase 2
AA403841	**3.0**	**Galectin 3 (Mac-2)**
AA466432	3.0	S100 calcium-binding protein A1
AA108857	**2.7**	**Prostaglandin D2 synthase (21 kDa, brain)**
AA119121	**2.7**	**Annexin A3**
AA119293	2.6	Small inducible cytokine A6
AA064307	**2.6**	**ESTs, highly similar to CD34**
AA259979	2.6	Angiotensinogen
AA396152	**2.5**	**ESTs, similar to CD44**
AA017875	2.5	ESTs, weakly similar to cytoskeletal P17 protein
AA122791	**2.4**	**Histocompatibility 2, Q region locus 7**
AA259959	**2.4**	**CD37**
AA261393	**2.4**	**ESTs, highly similar to complement C1r component**
W98963	**2.4**	**CD9**
AA253938	2.4	ESTs, moderately similar to hypothetical 167.8 KDa protein
W78651	2.3	Cystatin 3
W09925	2.3	Creatine kinase, brain
AA212780	2.3	Nip2l
AA175441	2.3	Glycoprotein galactosyltransferase alpha 1, 3
AA145820	2.3	ESTs, weakly similar to coded for by *C. elegans* cDNA yk13g5.3
AA538511	**2.2**	**Histocompatibility 2, L region**
AA237828	2.2	Protein S (alpha)
AA543497	2.2	Ciliary neurotropic factor
AA230451	2.2	Calgranulin A
W82159	**2.2**	**Fc receptor, IgG, low-affinity III**
W82946	**2.2**	**Benzodiazepine receptor, peripheral**
AA108928	**2.1**	**Secreted phosphoprotein 1 (Osteopontin)**
AA002514	2.1	Brain lipid-binding protein
AA003904	2.1	Thrombospondin 2
AA038657	2.1	TG interacting factor
W66661	2.1	ESTs, moderately similar to membrane-associated protein HEM-2
AA475774	**2.1**	**Cathepsin C**
AA275763	2.1	Uridine monophosphate kinase
AA063753	2.1	ATP-binding cassette 1
AA266002	2.0	B-cell leukemia/lymphoma 3
AA237378	2.0	Extracellular matrix protein 1
W83609	2.0	Retinol binding protein 1, cellular
AA145856	2.0	Repeat-family 3 gene
AA017918	2.0	ESTs, highly similar to dJ465N24.1
AA016374	**2.0**	**ESTs, highly similar to α-2-macroglobulin**
W62819	2.0	Neuronal protein 3.1
AA222201	2.0	Butyrate response factor 1
AA034857	2.0	RNA-binding motif protein 3
AA175510	2.0	RAB1, member RAS oncogene family
AA109684	2.0	Cytochrome P450, 4a10
W17771	2.0	Cathelin-like protein
AA212896	**2.0**	**EGF-like module sequence 1, similar to F4/80 antigen**
AA467383	2.0	ESTs, similar to α-crystallin-related protein
AA254511	2.0	ESTs, highly similar to Zinc finger protein 183
AA186012	**2.0**	**Histocompatibility 2, Q region locus 7**

Listed are known genes that are up-regulated by 2-fold or greater in the spinal cord of 4-month-old Sandhoff disease mice. The expression ratio was calculated by dividing fluorescence intensity (FI) of gene elements in Sandhoff disease mice by FI of gene elements in control mice. The genes in bold type are expressed in the macrophage/microglia lineage or are indicative of an inflammatory reaction. EST, expressed sequence tag.

were not detectable in cerebral cortex and cerebellum in 4-month-old mice even though glycolipid storage was abundant in these regions. In control mice, apoptotic neurons were not detected.

Messenger RNA Expression Profile in Sandhoff Disease Mice. In an attempt to understand the molecular basis underlying the neuronal apoptosis, we performed cDNA microarray analysis (20) to identify the changes in gene expression that accompanied the neuronal cell death in spinal cord. Spinal cord mRNA samples from 4-month-old wild-type and Sandhoff mice were labeled with Cy3 and Cy5 fluorescent dyes, respectively, and hybridized to a cDNA microarray containing 7,854 unique mouse gene sequences. Eighty-nine, or about 1% of the elements monitored, were expressed at a 2.0-fold or greater level in the spinal cord of the Sandhoff disease mice compared with spinal cord of control mice. Sixty-eight of these up-regulated elements were known genes (Table 1). The others represented, as yet, unidentified expressed sequence tags. Just 16 elements were down-regulated by 2.0-fold or more (not shown). The expression profile of up-regulated genes was dominated by genes characteristic of an inflammatory response. Many of these genes are expressed by the macrophage/microglia[§] lineage such as CD68 (21), Mac-1 α-subunit (22), galectin3 (Mac-2) (23), and epidermal growth factor-like module containing receptor similar to F4/80 antigen (24), macrophage-expressed gene 1 (25), annexin 3 (26), and the secreted phosphoprotein1 (osteopontin) (27). Other up-regulated genes were characteristic of macrophage/microglial activation. These included genes encoding cathepsin S (28), Fc receptor, complement components, and major histocompatibility complex 2 genes (29, 30).

The 16 genes found to be down-regulated by more than 2-fold included an expressed sequence tag clone highly homologous to mouse peripheral myelin protein (GenBank accession nos. W65570 and AA097191).

To confirm the microarray results, which indicated genes related to a macrophage-mediated inflammatory response were elevated, we measured the relative expression of a subset of these genes by real-time PCR (Table 2). Expression was determined in spinal cord at 1, 2, 3, and 4 months of age. Each of these genes showed a time-dependent increase of expression in Sandhoff mice compared with controls confirming the microarray results. Elevations in expression of the majority of the genes were seen as early as 1 or 2 months, indicating that the altered gene expression began before detectable neuronal apoptosis and acute disease symptoms.

Microglial Activation and Expansion. The gene expression profile of the spinal cord prompted us to undertake a histologic investigation to both confirm and characterize the possible activated microglial response during the disease process.

A survey of microglia in Sandhoff mice was performed at 1, 2, 3, and 4 months of age by using antibody to macrophage marker F4/80 and $GSIB_4$, which intensely stains activated microglia (16) (Fig. 2). In control mice, microglia had a ramified structure with fine processes—a morphology associated with a quiescent state (Fig. 2*b*). In Sandhoff mice at 1 month of age, only a few microglia were amoeboid in shape—a morphology associated with an activated state—and stained with $GSIB_4$. These cells were noted around the blood vessels in the spinal cord. At 2 months of age, activated microglia could be identified around the blood vessels throughout the CNS; however, activated microglia were rare in the parenchyma of the spinal cord, brainstem, and thalamus. At 3 months of age, amoeboid microglia were increased in number in parenchyma of spinal cord,

[§]Microglia will be defined operationally as cells of the macrophage lineage that are found in the CNS.

Table 2. Gene expression in spinal cord of Sandhoff disease mice

	1 M	2 M	3 M	4 M
B lymphocyte chemoattractant	1.3 ± 0.3	2.0 ± 0.7	27.6 ± 8.0	76.3 ± 30.0
Cathepsin S	1.5 ± 0.3	2.0 ± 0.5	4.2 ± 0.5	6.1 ± 0.3
CD68	1.7 ± 0.1	3.0 ± 0.7	10.7 ± 2.1	15.1 ± 1.6
F4/80	1.7 ± 0.1	2.8 ± 0.4	5.5 ± 1.3	5.0 ± 0.7
Macrophage-expressed gene 1	2.2 ± 0.3	3.4 ± 0.7	9.2 ± 1.4	14.2 ± 0.8
Mac-1 α-subunit	2.0 ± 0.3	5.5 ± 2.0	48.6 ± 7.9	39.7 ± 1.6
Galectin 3 (Mac-2)	1.6 ± 0.3	2.7 ± 0.6	14.2 ± 1.2	16.0 ± 0.3
Secreted phosphoprotein 1	1.0 ± 0.1	1.3 ± 0.2	2.9 ± 0.3	2.4 ± 0.3
Prostaglandin D2 synthase	1.9 ± 0.3	2.2 ± 0.6	2.3 ± 0.6	3.6 ± 1.2

The expression levels of mRNAs were measured by real-time PCR. The expression levels were standardized by expression levels of glyceraldehyde-3-phosphate dehydrogenase. The values represent relative expression levels of genes (fold-increase) in spinal cord of Sandhoff disease mice at 1, 2, 3, and 4 months (M) of age compared with age-matched control mice. Data are mean ± SEM ($n = 3$).

brainstem, and thalamus (Fig. 2*e*). At 4 months of age, the population of amoeboid microglial cells in these brain regions had expanded further (Fig. 2 *a*, *c*, and *e*). The activated status of the cells also was confirmed by the intense staining of the microglia with antibody to phosphotyrosine (31) and to the proinflammatory cytokine TNF-α (not shown). Amoeboid microglia were not found in the parenchyma of cerebellum or cerebral cortex of Sandhoff disease mice.

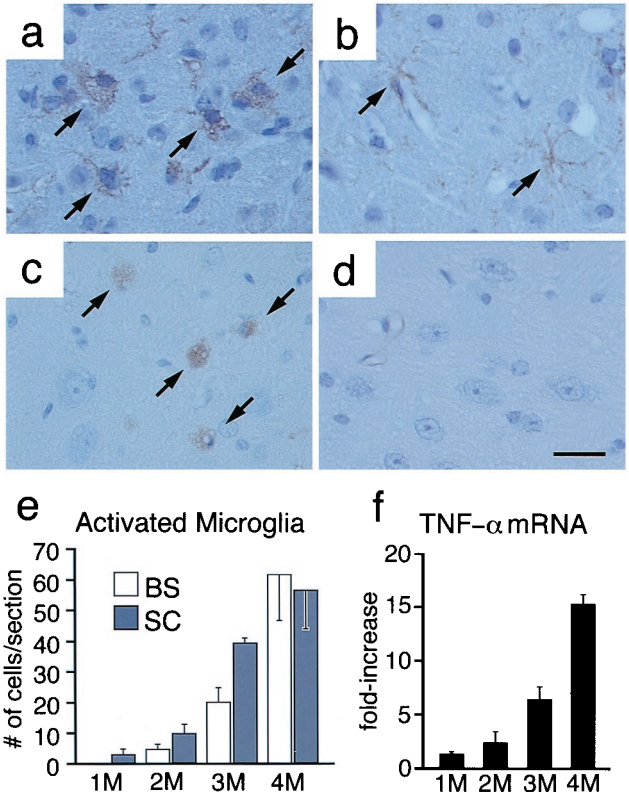

Fig. 2. Microglia activation and expansion in Sandhoff disease mice. Immunostaining with anti-F4/80 antibody shows amoeboid microglia in the brainstem of 4-month-old Sandhoff disease mouse (*a*) and ramified microglia in the brainstem of age-matched control mouse (*b*). Staining with $GSIB_4$ shows amoeboid microglia in the spinal cord of a 4-month-old Sandhoff disease mouse (*c*) but not in a control mouse (*d*). (Bar = 20 μm.) (e) Quantitation of $GSIB_4$-positive microglia in brainstem (BS) and spinal cord (SC) of Sandhoff mice. The $GSIB_4$-positive cells were counted in semisequential sections of brain and spinal cord. Data are mean ± SEM ($n = 3$–4). (*f*) TNF-α mRNA expression levels in the spinal cord of Sandhoff disease mice compared with age-matched control mice. (SD). Data are mean ± SEM ($n = 3$).

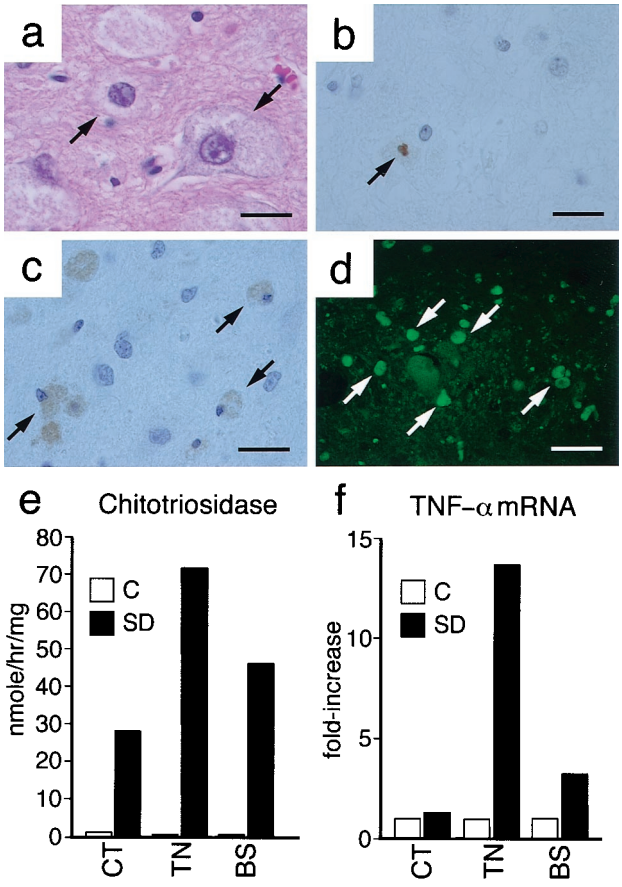

Fig. 3. Microglia activation and expansion in a Sandhoff disease patient. (*a*) Hematoxylin and eosin staining of section of thalamus from the Sandhoff disease patient. Arrows indicate neuronal cells with storage of gangliosides. (*b*) TUNEL staining of the cerebral cortex of the patient. Arrow indicates TUNEL-positive neuronal cells. (*c*) Immunostaining of thalamic nucleus with anti-CD68 antibody. Arrows indicate CD68-positive microglia. [Bar = 20 μm (*a*-*c*).] (*d*) Immunofluorescent staining of the cerebellum with antiphosphotyrosine antibody. Arrows indicate activated microglia intensely stained with antiphosphotyrosine antibody. (Bar = 50 μm.) (*e*) Chitotriosidase activity of brain regions from control (C) and from the Sandhoff disease patient (SD). The activity is elevated in the cerebral cortex (CT), thalamic nucleus (TN), and brainstem (BS) of a Sandhoff disease patient. (*f*) TNF-α mRNA expression levels in control (C) and in the Sandhoff disease patient (SD). The expression levels are elevated in thalamic nucleus (TN) and brainstem (BS) but not in the cerebral cortex (CT) of the Sandhoff disease patient.

TNF-α gene expression was determined in the spinal cord of Sandhoff disease mice by real-time reverse transcription–PCR. At 2 months of age, TNF-α levels were elevated by 2-fold over control mice. Expression was elevated 7-fold at 3 months and increased to 15-fold at 4 months of age (Fig. 2*f*).

Microglial Activation in a Sandhoff Disease Patient. To determine whether a comparable inflammatory reaction was present in the human disorder, brain samples from a Sandhoff disease patient were examined histologically and biochemically. Neurons throughout the brain of the patient were distended with ganglioside storage (Fig. 3*a*), and neuronal loss was evident. Apoptotic death was detected in the cortex, brainstem, thalamus, and cerebellum (Fig. 3*b*), as had been described previously (3).

MEDICAL SCIENCES

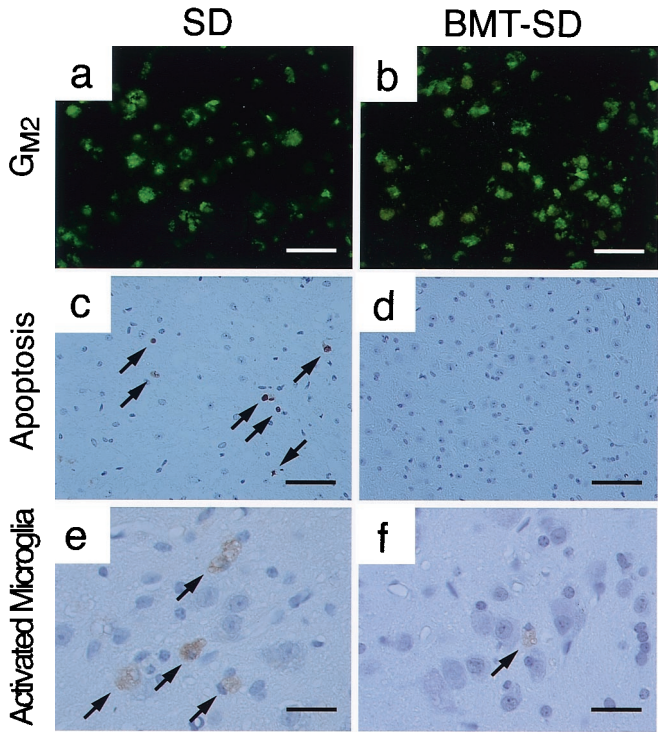

Fig. 4. Reduction of activated microglia, neuronal apoptosis, but not G_{M2} storage in bone marrow-transplanted Sandhoff disease mice. Untreated 4-month-old Sandhoff disease mouse [SD (*a*, *c*, and *e*)] and bone marrow-transplanted Sandhoff disease mouse [BMT-SD (*b*, *d*, and *f*)] were analyzed. (*a* and *b*) Immunostaining with anti-G_{M2} ganglioside antibody. (Bar = 50 μm.) (*c* and *d*) TUNEL staining of thalamic nuclei. Arrows indicate apoptotic cells. (Bar = 50 μm.) (*e* and *f*) Staining with GSIB4. Arrows indicate $GSIB_4$-positive cells. (Bar = 20 μm.)

Numerous CD68-positive microglia were found throughout the CNS of the Sandhoff disease patient (Fig. 3*c*). They were a plump, amoeboid shape, with inconspicuous processes. These cells immunostained intensely with antiphosphotyrosine antibody (Fig. 3*d*), indicating an activated state.

Chitotriosidase expression has been shown to be a marker for peripheral macrophage activation in Gaucher disease (19). We found extremely high levels of chitotriosidase activity in the brain samples of the Sandhoff disease patient with approximately 200-fold elevations in the thalamic nuclei and brainstem and with a 25-fold increase in the cerebral cortex, compared with control (Fig. 3*e*). Elevated TNF-α gene expression was found in the thalamic nucleus (≈14-fold) and brainstem (≈3-fold) (Fig. 3*f*).

Sandhoff Disease Mice Treated with BMT. BMT extends the lifespan of Sandhoff mice and ameliorates neurologic symptoms (15). Immunostaining of spinal cord, brainstem, and thalamus with antibody to G_{M2} ganglioside to visualize neuronal storage revealed no difference in staining intensity between untreated Sandhoff mice and those treated by BMT (Fig. 4 *a* and *b*). These results are in agreement with previous data that showed similar glycolipid levels in the CNS of BMT-treated and untreated Sandhoff mice (15). At 4 months of age, apoptotic death was virtually absent in the spinal cord, brainstem, and thalamus of BMT-treated Sandhoff mice compared with the abundant apoptosis in untreated mice (Fig. 4 *c* and *d*). In the spinal cord of 4-month-old untreated Sandhoff disease mice, amoeboid microglia were numerous. In BMT-treated Sandhoff mice, the activated, amoeboid microglia were present at a much lower density (Fig. 4 *e* and *f*). There was a 78% decrease in the number of activated microglia in spinal cord and a 91% decrease in brainstem of BMT-treated Sandhoff mice compared with untreated mice.

Discussion

After the initial onset of symptoms, the G_{M2} gangliosidoses are characterized by a precipitous neurodegenerative course, leading rapidly to death. Using a mouse model of Sandhoff disease, we studied the temporal relationship of neuronal apoptosis to disease progression. Before 3 months of age, the Sandhoff mice are relatively free of a disease phenotype. At about 3 months of age, the mice begin a rapid decline in motor function, culminating in a moribund condition by 4.5 months. We found that the first detectable neuronal apoptosis coincided with the beginning of the rapid, degenerative phase of the disease. By 4 months, near the nadir of the disease process, the apoptotic neurons were relatively frequent. Although glycolipid storage occurred in virtually all neurons, apoptotic cell death was concentrated in caudal regions of the CNS—in spinal cord, brainstem, and thalamus.

The pattern of genes overexpressed in the spinal cord of symptomatic Sandhoff disease mice indicated the presence of activated microglia. Histological evaluation and gene expression measurements confirmed their presence as early as 1–2 months of age and with elevated levels at 3 months of age. The results indicate that activated microglia were not simply a reaction to massive cell death at the terminal stage of the disease. Activated microglia were present in the same regions—spinal cord, brainstem, and thalamus—that eventually demonstrated a high degree of cell death. These activated microglia produced TNF-α, a proinflammatory cytokine that has been shown to have both neurotoxic and neuroprotective effects (32, 33).

Although extremely helpful in directing our attention to the intense inflammatory response, the microarray data mirrored the information gleaned from the histologic analysis of the Sandhoff disease mice. The microarray data were also provided with a set of genes that allowed for the temporal quantitation of the inflammatory reaction during the disease process and confirmed an early macrophage expansion. Ultimately, these overexpressed genes may be useful as surrogate markers to chart the course of the disease.

In Sandhoff disease mice, BMT improves neurological symptoms and prolongs lifespan (15). The procedure results in the infiltration of β-hexosaminidase-positive microglia into predominately the same regions that suffer from the highest degree of apoptotic cell death in untreated mice (34). Microglial activation and neuronal cell death was largely suppressed by BMT. The clinical improvement does not appear to be a result of the removal of a radiosensitive cell by the irradiation given during BMT because Sandhoff mice transplanted with Sandhoff bone marrow showed no neurologic improvement and no lengthening of lifespan (data not shown). In other storage diseases, BMT has been shown to reduce neuronal storage through transfer of lysosomal enzymes into neurons by infiltrating microglia (35, 36). In BMT-treated Sandhoff disease mice, β-hexosaminidase-positive neurons could not be detected although enzyme-positive microglia could be found (34). A decrease in neuronal G_{M2} ganglioside storage in spinal cord and brainstem was not detectable by immunostaining.

Based on our results, we suggest a pathogenic mechanism in which a relentlessly increasing inflammatory response actively participates in a pathway of acute neurodegeneration (Fig. 5). In this model, glycolipid accumulation is the primary insult to neurons, which undoubtedly causes dysfunction and damage. Microglia recognize damaged and dying neurons and remove them by phagocytosis. Such a process may be expected to elicit an inflammatory reaction to some degree. However, the process is greatly exacerbated by the inability of the microglia to degrade the endocytosed glycolipids because of their own enzyme deficiency. As a result, blood-borne microglial precursors are re-

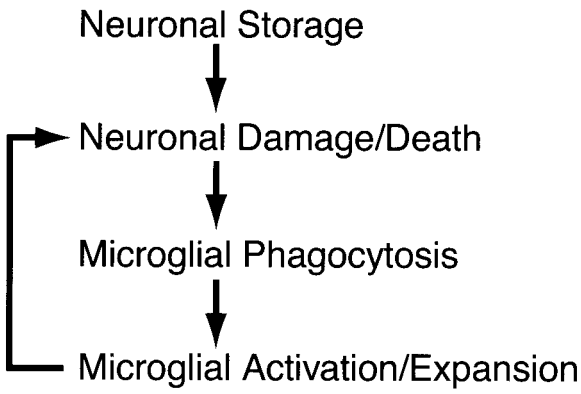

Fig. 5. Model for acute neurodegeneration in G_{M2} gangliosidoses. In this model, storage of G_{M2} ganglioside and related glycolipids causes primary neuronal damage. Microglia recognize damaged and dying neurons and remove them by phagocytosis. The inability of the enzyme-deficient microglia to catabolize endocytosed glycolipid leads to their activation and the recruitment of additional microglial precursors from blood. The large expansion of the activated microglial population produces neurotoxic mediators, which provides an additional insult to the neurons already stressed by glycolipid storage, resulting in widespread neuronal apoptosis. BMT may disrupt this pathway through the introduction of normal microglia into the CNS. These normal microglia can effectively remove the neurons damaged by storage and, thus, temporarily suppress the recruitment and expansion of the activated microglial population.

cruited continuously by activated, lipid-laden microglia in the CNS in an attempt to manage the neuronal damage. The expansion of activated microglia could trigger cell death in neurons already compromised by excessive storage through expression of neurotoxic cytokines and other mediators (30).

BMT suppresses this inflammatory pathogenic process by the infiltration of normal microglia into the CNS (34, 37). These enzyme-competent microglia are fully functional and are able to remove damaged storage neurons. The ability of functional microglia to handle the neuronal damage suppresses the explosive expansion of activated microglia seen in untreated mice. This retards the neurodegenerative process by reducing the neuronal insult from the excessive inflammatory response.

Neuronal apoptosis has been shown to underlie several neurodegenerative diseases including Alzheimer's disease (4, 5), prion diseases (6, 7), and HIV-dementia (8, 38). In each, there is strong evidence for an inflammatory response involving microglial activation that leads to neuronal apoptosis. Activated microglia express potentially neurotoxic cytokines and substances such as TNF-α, proteases, oxyradicals, and small reactive molecules (30). Our study on the human case of Sandhoff disease was, by necessity, at the terminal stage of the disorder. However, intense microglial activation was detected along with elevated TNF-α levels. It now will be of interest to determine whether other storage diseases with a neurodegenerative component also develop an aggressive inflammatory response early in the disease process.

Because of the relentless progression of neuronal glycolipid storage, antiinflammatory agents alone would not be expected to halt the disease process in the infantile G_{M2} gangliosidoses. However, combination therapies that could lower the storage burden and the inflammatory process may be contemplated. Finally, it will be important to investigate the pathogenesis of the more slowly progressing, late-onset forms of Tay-Sachs and Sandhoff disease for an inflammatory component. If present, then a therapy to reduce the inflammatory response may be beneficial in these chronic diseases.

We are grateful to Jennifer Reed and April Howard for technical assistance.

1. Neufeld, E. F. (1991) *Annu. Rev. Biochem.* **60,** 257–280.
2. Gravel, R. A., Clarke, J. T. R., Kabak, M. M., Mahhuran, D., Sandhoff, K. & Suzuki, K. (1995) in *The Metabolic Basis of Inherited Disease*, eds. Scriver, C. R., Beaudet, A. L., Sly, W. S. & Valle, D. (McGraw–Hill, New York), pp. 2839–2879.
3. Huang, J. Q., Trasler, J. M., Igdoura, S., Michaud, J., Hanal, N. & Gravel, R. A. (1997) *Hum. Mol. Genet.* **6,** 1879–1885.
4. Lassmann, H., Bancher, C., Breitschopf, H., Wegiel, J., Bobinski, M., Jellinger, K. & Wisniewski, H. M. (1995) *Acta. Neuropathol.* **89,** 35–41.
5. Su, J. H., Anderson, A. J., Cummings, B. J. & Cotman, C. W. (1994) *NeuroReport* **5,** 2529–2533.
6. Giese, A., Brown, D. R., Groschup, M. H., Feldmann, C., Haist, I. & Kretzschmar, H. A. (1998) *Brain Pathol.* **8,** 449–457.
7. Gray, F., Chretien, F., Adle-Biassette, H., Dorandeu, A., Ereau, T., Delisle, M. B., Kopp, N., Ironside, J. W. & Vital, C. (1999) *J. Neuropathol. Exp. Neurol.* **58,** 321–328.
8. Shi, B., De Girolami, U., He, J., Wang, S., Lorenzo, A., Busciglio, J. & Gabuzda, D. (1996) *J. Clin. Invest.* **98,** 1979–1990.
9. Gehrmann, J., Matsumoto, Y. & Kreutzberg, G. W. (1995) *Brain Res. Brain Res. Rev.* **20,** 269–287.
10. Williams, A., Lucassen, P. J., Ritchie, D. & Bruce, M. (1997) *Exp. Neurol.* **144,** 433–438.
11. Combs, C. K., Johnson, D. E., Cannady, S. B., Lehman, T. M. & Landreth, G. E. (1999) *J. Neurosci.* **19,** 928–939.
12. Bianca, V. D., Dusi, S., Bianchini, E., Dal Pra, I. & Rossi, F. (1999) *J. Biol. Chem.* **274,** 15493–15499.
13. Aoki, T., Kobayashi, K. & Isaki, K. (1999) *Clin. Neuropathol.* **18,** 51–60.
14. Sango, K., Yamanaka, S., Hoffmann, A., Okuda, Y., Grinberg, A., Westphal, H., McDonald, M. P., Crawley, J. N., Sandhoff, K., Suzuki, K., *et al.* (1995) *Nat. Genet.* **11,** 170–176.
15. Norflus, F., Tifft, C. J., McDonald, M. P., Goldstein, G., Crawley, J. N., Hoffmann, A., Sandhoff, K., Suzuki, K. & Proia, R. L. (1998) *J. Clin. Invest.* **101,** 1881–1888.
16. Streit, W. J. (1990) *J. Histochem. Cytochem.* **38,** 1683–1686.
17. Liu, Y., Wada, R., Kawai, H., Sango, K., Deng, C., Tai, T., McDonald, M. P., Araujo, K., Crawley, J. N., Bierfreund, U., *et al.* (1999) *J. Clin. Invest.* **103,** 497–505.
18. Pulford, K. A., Rigney, E. M., Micklem, K. J., Jones, M., Stross, W. P., Gatter, K. C. & Mason, D. Y. (1989) *J. Clin. Pathol.* **42,** 414–421.
19. Hollak, C. E., van Weely, S., van Oers, M. H. & Aerts, J. M. (1994) *J. Clin. Invest.* **93,** 1288–1292.
20. Schena, M., Shalon, D., Heller, R., Chai, A., Brown, P. O. & Davis, R. W. (1996) *Proc. Natl. Acad. Sci. USA* **93,** 10614–10619.
21. Ulvestad, E., Williams, K., Bjerkvig, R., Tiekotter, K., Antel, J. & Matre, R. (1994) *J. Leukocyte Biol.* **56,** 732–740.
22. Akiyama, H. & McGeer, P. L. (1990) *J. Neuroimmunol.* **30,** 81–93.
23. Pesheva, P., Urschel, S., Frei, K. & Probstmeier, R. (1998) *J. Neurosci. Res.* **51,** 49–57.
24. McKnight, A. J., Macfarlane, A. J., Dri, P., Turley, L., Willis, A. C. & Gordon, S. (1996) *J. Biol. Chem.* **271,** 486–489.
25. Spilsbury, K., O'Mara, M. A., Wu, W. M., Rowe, P. B., Symonds, G. & Takayama, Y. (1995) *Blood* **85,** 1620–1629.
26. Le Cabec, V., Russo-Marie, F. & Maridonneau-Parini, I. (1992) *Biochem. Biophys. Res. Commun.* **189,** 1471–1476.
27. Miyazaki, Y., Setoguchi, M., Yoshida, S., Higuchi, Y., Akizuki, S. & Yamamoto, S. (1990) *J. Biol. Chem.* **265,** 14432–14438.
28. Petanceska, S., Canoll, P. & Devi, L. A. (1996) *J. Biol. Chem.* **271,** 4403–4409.
29. McGeer, P. L., Itagaki, S., Tago, H. & McGeer, E. G. (1987) *Neurosci. Lett.* **79,** 195–200.
30. Minghetti, L. & Levi, G. (1998) *Prog. Neurobiol.* **54,** 99–125.
31. Karp, H. L., Tillotson, M. L., Soria, J., Reich, C. & Wood, J. G. (1994) *Glia* **11,** 284–290.
32. Merrill, J. E. & Benveniste, E. N. (1996) *Trends Neurosci.* **19,** 331–338.
33. Tarkowski, E., Blennow, K., Wallin, A. & Tarkowski, A. (1999) *J. Clin. Immunol.* **19,** 223–230.
34. Oya, Y., Proia, R. L., Norflus, F., Tifft, C. J., Langamann, C. & Suzuki, K. (2000) *Acta. Neuropathol.* **99,** 161–168.
35. Hoogerbrugge, P. M., Suzuki, K., Poorthuis, B. J., Kobayashi, T., Wagemaker, G. & van Bekkum, D. W. (1988) *Science* **239,** 1035–1038.
36. Walkley, S. U., Thrall, M. A., Dobrenis, K., Huang, M., March, P. A., Siegel, D. A. & Wurzelmann, S. (1994) *Proc. Natl. Acad. Sci. USA* **91,** 2970–2974.
37. Kennedy, D. W. & Abkowitz, J. L. (1997) *Blood* **90,** 986–993.
38. Adle-Biassette, H., Chretien, F., Wingertsmann, L., Hery, C., Ereau, T., Scaravilli, F., Tardieu, M. & Gray, F. (1999) *Neuropathol. Appl. Neurobiol.* **25,** 123–133.